New Information on Water Interfacial Structure Revealed by Phase-Sensitive Surface Spectroscopy

Victor Ostroverkhov,[1] Glenn A. Waychunas,[2] and Y. R. Shen[1]
[1]Department of Physics, University of California, Berkeley, California, 94720, USA
[2]Earth Sciences Division, Lawrence Berkeley National Laboratory, One Cyclotron Road, Berkeley, California, 94720, USA
(Received 30 August 2004; published 2 February 2005)

A phase-sensitive sum-frequency vibrational spectroscopic technique is developed to study interfacial water structure of water/quartz interfaces. Measurements allow deduction of both real and imaginary parts of the surface nonlinear spectral response, revealing an unprecedentedly detailed picture of the net polar orientations of the water species at the interface. The orientations of the icelike and liquidlike species appear to respond very differently to the bulk pH change indicating the existence of different surface sites on quartz with different deprotonation pK values.

DOI: 10.1103/PhysRevLett.94.046102 PACS numbers: 68.08.De, 42.65.Ky, 68.43.Fg

Numerous physical, chemical, and biological processes of great importance are controlled or initiated at aqueous interfaces. Many of these are strongly affected by the interfacial water structure, and this has aroused great interest among researchers in various disciplines [1]. However, despite extensive theoretical and experimental investigation in the past, our knowledge of water interfacial structure at the molecular level is still very limited. Recently, x-ray spectroscopy [2], atomic force microscopy [3], and sum-frequency vibrational spectroscopy (SFVS) [4–8] have been developed to study water interfaces. Among them, SFVS is most attractive because of its ability to provide vibrational spectra of the interfaces that can be directly related to the interfacial structures. Using the technique, water species with liquidlike, icelike, and free hydroxyl structures forming a hydrogen-bonding network in the interfacial region have been identified.

While the observed SF vibrational spectra of water interfaces by different groups are generally similar, there is considerable disagreement in spectral interpretation and interface speciation. Part of the problem arises because the conventional SFVS technique does not provide information on the polar orientations of various interfacial species. Such information is actually inherent in SFVS if one would be able to measure both the intensity and the phase of the sum-frequency signal. Here, we describe such a complete SFVS measurement and its application to water/α-quartz interfaces, revealing an unprecedented detailed picture of the water interfacial structure. In particular, we discover that the orientations of icelike and liquidlike water species respond very differently to protonation and deprotonation at the surface.

In ordinary SFVS, two input beams at ω_1 and ω_2 overlap at an interface and generate a surface-specific sum-frequency output in transmission or reflection [9]. The signal is proportional to the absolute square of the surface nonlinear susceptibility, $|\chi_S^{(2)}(\omega = \omega_1 + \omega_2)|^2$. Resonant enhancement of $|\chi_S^{(2)}(\omega = \omega_1 + \omega_2)|$ as ω_2 scans over vibrational resonances leads to a vibrational spectrum. For water interfaces, the vibrational spectra generally exhibit in the OH stretch region a liquidlike peak at $\sim$3400 cm^{-1} and an icelike peak at $\sim$3200 cm^{-1} for the bonded OH stretches, indicating that the interfacial water molecules form a hydrogen-bonding network with intermingled ordered (icelike) and disordered (liquidlike) structures. The free OH peak at $\sim$3700 cm^{-1} normally present at hydrophobic interfaces is suppressed at hydrophilic interfaces (e.g., quartz) [4]. Successful fitting of the spectra by more than three resonant peaks has led some researchers to believe that there are also additional water interfacial species [5]. Others have attributed the liquidlike peak to water molecules next to the surface and the icelike peak to water molecules at a greater distance away from the surface aligned by the surface field [6]. Earlier, Eisenthal and co-workers [10], using second-harmonic generation to probe water/silica interfaces, concluded that there exist two different surface sites that influence the water interfacial structure (possible existence of two silanol surface sites was first proposed by Allen *et al.* [11]). Surface charging by deprotonation at the two sites is different, resulting in different field-induced responses from the interfacial water. All the aforementioned results and interpretations are somewhat conflicting and have rendered the picture of interfacial water structure rather confusing. On the theoretical side, molecular dynamics simulations have been fairly successful, but they have not provided sufficient detail to help resolve among different interpretations [12]. It is clear that more molecular-level information about the interfaces is needed, and knowledge of the polar orientations of interfacial water molecules associated with the icelike and liquidlike peaks will help. This can be obtained from measuring the phases Φ of $\chi_S^{(2)}(\omega = \omega_1 + \omega_2) = |\chi_S^{(2)}|\exp(i\Phi)$, over the spectral range. A 180 ° phase reversal of $\chi_S^{(2)}(\omega = \omega_1 + \omega_2)$ indicates that the polar orientation of the contributing water molecules has flipped.

It is well known that one can use interference methods to measure the phase of a nonlinear susceptibility, but measurements are usually carried out with only a set of fixed

input/output frequencies [4,13]. We report here phase measurement over the SF vibrational spectra of the water/α-quartz interfaces in the OH stretch range with different bulk pH values. It is based on interference of sum-frequency generation (SFG) from the water interface and the bulk α-quartz. In this case, the overall SF signal is given by [9]

$$S(\omega; \hat{e}, \hat{e}_1, \hat{e}_2) \propto |\chi^{(2)}_{\text{eff}}|^2 I(\omega_1) I(\omega_2)$$
$$\chi^{(2)}_{\text{eff}} = L\hat{e} \cdot \left[\vec{\chi}^{(2)}_S + \frac{\vec{\chi}^{(2)}_B}{i\Delta k} \right] : (\hat{e}_1 L_1)(\hat{e}_2 L_2), \tag{1}$$

where $\hat{e}_i$, $I(\omega_i)$, and L_i are, respectively, the polarization unit vector, the incoming beam intensity, and the transmission Fresnel coefficient at ω_i, $\vec{\chi}^{(2)}_S$ and $\vec{\chi}^{(2)}_B$ are rank-3 nonlinear susceptibility tensors for the interface and the quartz bulk, and $\Delta k = |\vec{k} - \vec{k}_1 - \vec{k}_2|$ is the wave-vector mismatch of SFG along the surface normal direction. Since α-quartz is of D_3 symmetry without an inversion center, $\vec{\chi}^{(2)}_B$ is nonzero and dominated by tensor elements $\chi^{(2)}_{B,XXX} = -\chi^{(2)}_{B,XYY} = -\chi^{(2)}_{B,YXY} = -\chi^{(2)}_{B,YYX}$, where $\hat{X}$, $\hat{Y}$, and $\hat{Z}$ are the three crystalline axes.

For SFG from water/α-quartz(0001) interfaces, $\vec{\chi}^{(2)}_B$ has a threefold symmetry about the surface normal ($\hat{z}||\hat{Z}$). Rotating the cyrstalline X axis of the quartz crystal away from the incident plane (zx) of light by an angle of 30° (inset of Fig. 1) yields $\chi^{(2)}_B(SSP) = 0$, where SSP refers to S-, S-, and P-polarized SF output, visible input, and IR input, respectively. Then if the SF polarization is deviated by a small angle $\pm\gamma$ from the S polarization, we find

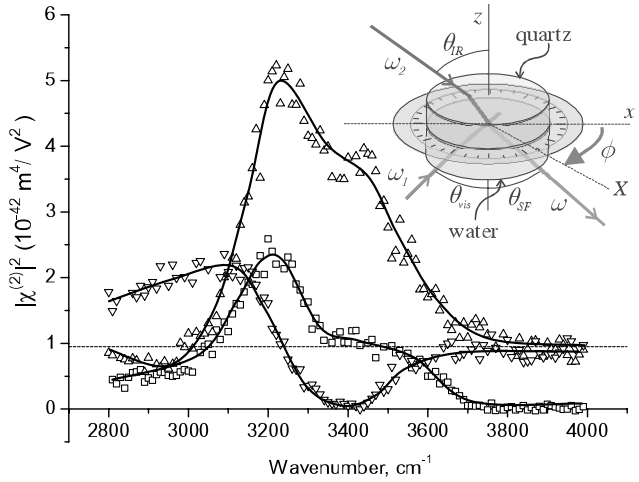

FIG. 1. A typical set of measured spectra for water/silica interfaces taken with $S_\gamma SP$ polarization combination and bulk pH = 6.5. The three spectra were taken with the output polarization set at $\gamma = 0$ (□), and $\gamma = \pm 5°$ (△ and ▽). The dotted horizontal line denotes the signal from bulk contribution alone, $S_Q(\gamma = \pm 5°)$. The inset depicts the sample stage and beam geometry.

$$S(\pm\gamma) = A|\chi^{(2)}_{S\gamma} \pm i\tilde{\chi}^{(2)}_{B\gamma}|^2$$
$$= A[|\chi^{(2)}_{S\gamma}|^2 + |\tilde{\chi}^{(2)}_{B\gamma}|^2 \pm 2|\chi^{(2)}_{S\gamma}\tilde{\chi}^{(2)}_{B\gamma}| \sin\Phi]$$
$$\tilde{\chi}^{(2)}_{B\gamma} \equiv \gamma \frac{\chi^{(2)}_{B,XXX}}{\Delta k} \cos\theta_{\text{IR}} \cos\theta_{\text{SF}} \tag{2}$$
$$\chi^{(2)}_{S\gamma} \equiv \hat{e}_{S\gamma} \cdot \vec{\chi}^{(2)}_S : \hat{e}_S \hat{e}_P = \chi^{(2)}_S \cos\gamma,$$

where A is a constant, θ_{IR} and θ_{SF} are angles of incidence at ω_2 and ω, respectively, and Φ is the phase of $\chi^{(2)}_S$ relative to that of bulk quartz. Since $\chi^{(2)}_{B\gamma}$ should be real in the OH stretch range where quartz is transparent, Φ is simply the phase of $\chi^{(2)}_S$ and is expected to vary over vibrational resonances of $\chi^{(2)}_S$. Now that $S(\pm|\gamma|)$ and $S_Q(\gamma) \equiv A|\tilde{\chi}^{(2)}_{B\gamma}|^2$ for a given γ as well as $S(\gamma = 0) = A|\chi^{(2)}_S|^2$ can be independently measured, we can deduce Φ from

$$\Phi = \sin^{-1}\left[\frac{S(|\gamma|) - S(-|\gamma|)}{4\sqrt{S(0)S_Q(\gamma)}\cos\gamma} \right]. \tag{3}$$

The experimental arrangement for SFVS was the same as that described in Ref. [14], and is schematically shown in the inset of Fig. 1. The α-quartz(0001) sample was cleaned in the usual way [14]. The sample was immersed in water with repeatedly varying pH prior to the measurement until the surface reached a nearly equilibrium state. With repeated cycling, the spectra became progressively more similar to those of water/fused quartz interfaces; the (0001)quartz surface appeared to have been affected by local dissolution. The sample was then properly oriented to $\phi = 30°$. For each bulk pH value, we took a series of spectra: one with the SSP polarization combination, and another two with $S_\gamma SP$ and $\gamma = \pm 5°$. The value of $S_Q(\gamma)$ was obtained from measurement of the dry quartz sample. An example is shown in Fig. 1 for pH = 6.5. The measurements were repeated for pH increasing from 1.5 to 11.5. The spectra of $\chi^{(2)}_S(\omega_2)$, Re$[\chi^{(2)}_S(\omega_2)]$, and Im$[\chi^{(2)}_S(\omega_2)]$ at different pH were then deduced from the measured spectra using Eq. (3). Figure 2 shows three sets of representative spectra of $|\chi^{(2)}_S(\omega_2)|$, Re$[\chi^{(2)}_S(\omega_2)]$, and Im$[\chi^{(2)}_S(\omega_2)]$ at different pH, among which is the set for pH = 6.5 deduced from the raw spectra in Fig. 1.

The spectra of $|\chi^{(2)}_S(\omega_2)|$ in Fig. 2 resemble those of water/fused silica interfaces [4,14], while those of Re$[\chi^{(2)}_S(\omega_2)]$ and Im$[\chi^{(2)}_S(\omega_2)]$ display variations in both amplitude and sign with pH. Here, we focus on the spectra of Im$[\chi^{(2)}_S(\omega_2)]$ because they are more informative. As shown in Fig. 3, we can decompose each spectrum of Im$[\chi^{(2)}_S(\omega_2)]$ in Fig. 2 into two components: one assumes the same spectral profile as that of infrared absorption of bulk liquid water [15] with a peak at 3400 cm^{-1} and fits

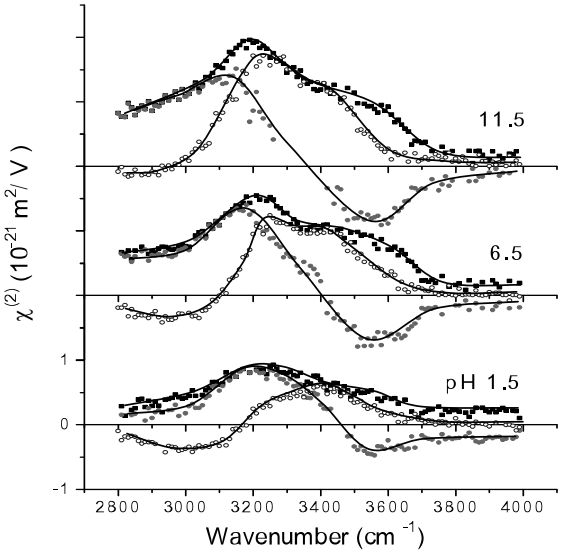

FIG. 2. The magnitude (■) and the real (•) and imaginary (○) parts of the nonlinear susceptibility of interfacial water, $\chi_S^{(2)}$, versus the input infrared frequency deduced from the measured sum-frequency spectra for three representative pH values of the aqueous solution. The solid curves are a guide to the eye.

the high-frequency end of the spectrum; the other takes up the remaining portion that fits the low-frequency end of the spectrum [Fig. 3(a)]. The uncertainty in such decomposition is less than 10%. The high-frequency component, usually labeled as the liquidlike peak, first increases in strength with increase of pH and begins to show saturation at $p\mathrm{H} \sim 4.0$ [see Fig. 3(c)]. The low-frequency component, usually labeled as the icelike peak, first appears as a negative peak centered at $\sim$3050 cm^{-1} at low pH, but reverts to a dominant positive peak centered at $\sim$3200 cm^{-1} at high pH. It can be further decomposed into two peaks, one at $\sim$3000 cm^{-1} with a full width at half maximum (FWHM) of 250 cm^{-1}, and the other at $\sim$3200 cm^{-1} with a FWHM of 170 cm^{-1} [Fig. 3(b)]. As pH increases, the higher-frequency peak first appears negative but gradually changes into a positive peak while the lower-frequency peak remains negative but shrinks. Variations of the two peak strengths with pH are also plotted in Fig. 3(c). We note that the spectra of quartz/water interfaces always showed some fluctuations and hysteresis with respect to increasing and decreasing pH, but the trend described above does not change.

The results provide the following detailed physical picture of the water/quartz interface. The quantity $\mathrm{Im}[\chi_S^{(2)}(\omega_2)]$ is a measure of net polar orientation of water molecules; positive and negative $\mathrm{Im}[\chi_S^{(2)}(\omega_2)]$ refer to molecular orientations with H and O facing the quartz surface, respectively. Figure 3 shows that the net polar orientations of water molecules in the more disordered liquidlike regions and the more ordered icelike regions are different and respond differently to deprotonation of

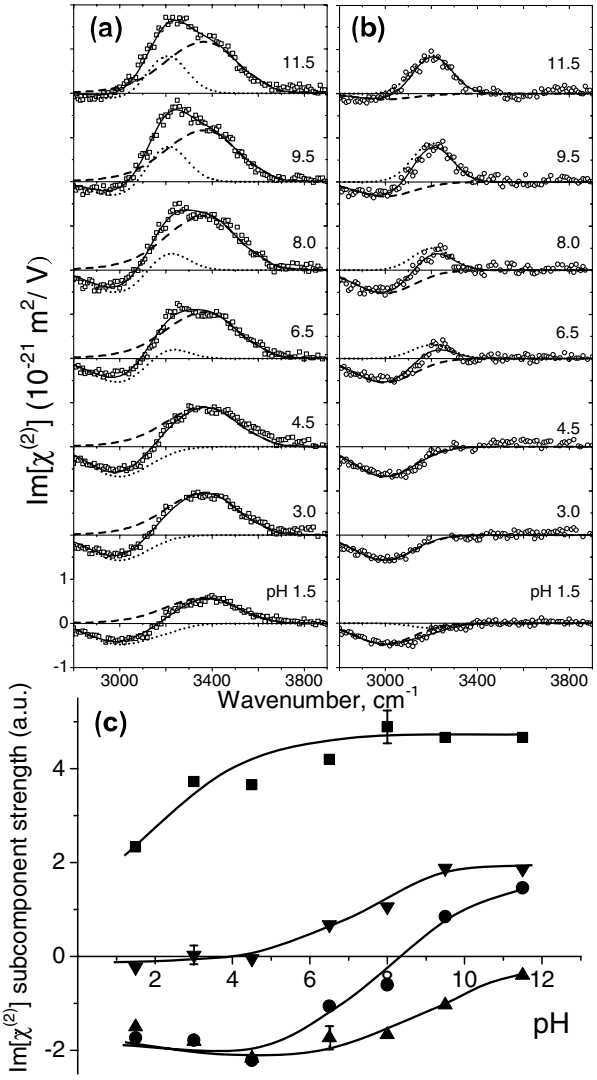

FIG. 3. (a) Decomposition of spectra of $\mathrm{Im}[\chi_S^{(2)}]$ (open squares and solid line) for different pH into a liquidlike component (dashed line) and icelike component (dotted line). (b) The icelike component (open circles and solid line) further decomposed into two subcomponents (dashed and dotted lines). For $p\mathrm{H} = 3.0$ and 4.5, the dashed line coincides with the solid line as the high-frequency subcomponent (dotted line) of the icelike peak has approximately zero strength. (c) Strengths versus pH of the liquidlike component (■), the 3000 cm^{-1} (▲), and the 3200 cm^{-1} subcomponent (▼) of the icelike component, as well as the overall integrated strength of the icelike component (•). The curves are a guide to the eye.

the quartz surface by increasing pH. At very low pH, the quartz surface passivated by H is nearly neutral ($\mathrm{SiO}^- + \mathrm{H}^+ \rightarrow \mathrm{SiOH}$), and interfacial water molecules would prefer to have their oxygen bound to the surface. This is true for molecules in the icelike regions. However, molecules in the liquidlike region still appear to have a net polar orientation with H facing the quartz surface. Thus there must exist on the quartz surface a significant number of surface sites that are deprotonated ($\mathrm{SiOH} \rightarrow \mathrm{SiO}^- + \mathrm{H}^+$) even at

very low pH; molecules in the less ordered liquidlike regions are more likely to bind to these local sites, leading to the observed net polar orientation. As pH increases, the quartz surface becomes more deprotonated (and negatively charged with a resulting surface field), and so there will be more water molecules with their H bound to the surface. As seen in Fig. 3, the net polar orientation in the liquidlike regions first increases with pH and then begins to saturate at $p\mathrm{H} \sim 4.0$. In the icelike regions, the change only becomes appreciable at $p\mathrm{H} \sim 4.5$, and then as pH increases, the net polar orientation of molecules flips from oxygen toward the surface to hydrogen toward the surface, with those more loosely bound to neighbors (as signified by higher stretch frequencies) reoriented first. Saturation of reorientation begins to set in at $p\mathrm{H} \sim 9.5$. These results indicate that there exist two types of surface sites with different deprotonation activities (different pK values), in agreement with the work of Eisenthal and co-workers [10]. The icelike regions seem to be associated with surface sites that are less easily deprotonated. Figure 3 shows that molecules contributing to the low-frequency subcomponent of the icelike peak always have a net polar orientation with oxygen facing the surface. This suggests that even at very high pH there are molecules bound to surface sites that remain protonated. Previous SFVS measurements of different water/oxide interfaces have found that the interfacial water spectra are qualitatively similar for all oxides [7]. Therefore, although our experimental study was limited to water/quartz interfaces, the general picture presented above is expected to be applicable to other water/oxide interfaces.

In summary, we have used a novel phase-sensitive SFVS technique to obtain the structure of the water/quartz interface in unprecedented detail. The interfacial water molecules appear to form a hydrogen-bonding network with intermingled regions of ordered and disordered structure (similar to the structure of systems undergoing an order-disorder transition [16]). Those in the ordered (disordered) regions giving rise to the icelike (liquidlike) peak in the spectra are closely associated with surface sites that possess a higher (lower) pK value for deprotonation. Increasing deprotonation of the surface sites induces more and more molecules in both regions to reorient with H facing the surface. However, at very low and very high pH values, residual deprotonated and protonated surface sites seem to exist in the disordered and ordered regions, respectively. This work shows that while the spectrum of water may look similar at different interfaces, the net orientation and polarization of water molecules can be very different. It further implies that potentially large differences in interfacial water properties may occur with subtle changes on the underlying solid surface, a connection that cannot be evaluated thoroughly without phase-sensitive SF vibrational spectroscopy. We expect that the new results would enable stringent testing of molecular-level theories or molecular dynamics simulations of water interfacial structure.

This work was supported by the STC Program of the National Science Foundation under Agreement No. CTS-0120978. G. A. W. was supported by the U. S. Department of Energy, Office of Basic Energy Sciences—Chemical Sciences, Geosciences, and Biosciences Division through the Lawrence Berkeley National Laboratory.

[1] G. W. Robinson, S. B. Zhu, S. Singh, and M. W. Evans, *Water in Biology, Chemistry, and Physics* (World Scientific, Singapore, 1996); G. E. Brown *et al.*, Chem. Rev. **99**, 77 (1999); *Water in Biomaterials Surface Science*, edited by M. Morra (John Wiley & Sons, New York, 2001); D. Marx, Science **303**, 634 (2004); B. C. Garrett, Science **303**, 1146 (2004); G. E. Brown, Science **294**, 67 (2001).

[2] P. S. Pershan, Physica A (Amsterdam) **200**, 50 (1993); M. F. Toney *et al.*, Nature (London) **368**, 444 (1994); K. R. Wilson *et al.*, J. Chem. Phys. **117**, 7738 (2002); M. F. Reedijk *et al.*, Phys. Rev. Lett. **90**, 066103 (2003).

[3] T. Mitsui *et al.*, Science **297**, 1850 (2002).

[4] Q. Du, R. Superfine, E. Freysz, and Y. R. Shen, Phys. Rev. Lett. **70**, 2313 (1993); Q. Du, E. Freysz, and Y. R. Shen, Science **264**, 826 (1994); Phys. Rev. Lett. **72**, 238 (1994).

[5] G. L. Richmond, Chem. Rev. **102**, 2693 (2002).

[6] M. C. Gurau *et al.*, Chem. Phys. Chem. **4**, 1231 (2003).

[7] M. S. Yeganeh, S. M. Dougal, and H. S. Pink, Phys. Rev. Lett. **83**, 1179 (1999); S. Kataoka *et al.*, Langmuir **20**, 1662 (2004).

[8] L. F. Scatena, M. G. Brown, and G. L. Richmond, Science **292**, 908 (2001); D. F. Liu, G. Ma, L. M. Levering, and H. C. Allen, J. Phys. Chem. B **108**, 2252 (2004); M. J. Shultz, S. Baldelli, C. Schnitzer, and D. Simonelli, J. Phys. Chem. B **106**, 5313 (2002).

[9] Y. R. Shen, in *Frontier in Laser Spectroscopy*, edited by T. W. Hansch and M. Inguscio (North Holland, Amsterdam, 1994), pp. 139–165.

[10] S. W. Ong, X. L. Zhao, and K. B. Eisenthal, Chem. Phys. Lett. **191**, 327 (1992).

[11] L. H. Allen, E. Matijevic, and L. Meties, J. Inorg. Nucl. Chem. **33**, 1293 (1971).

[12] A. Morita and J. T. Hynes, J. Phys. Chem. B **106**, 673 (2002); J. Puibasset and R. J. M. Pellenq, J. Chem. Phys. **119**, 9226 (2003); I. F. W. Kuo and C. J. Mundy, Science **303**, 658 (2004).

[13] Phase measurement over a broad spectrum of $\chi^{(2)}(\omega)$ has only been reported on electronic spectra obtained by optical second-harmonic generation. See S. Janz and Z. H. Lu, J. Opt. Soc. Am. B **14**, 1647 (1997); P. T. Wilson *et al.*, Opt. Lett. **24**, 496 (1999).

[14] V. Ostroverkhov, G. A. Waychunas, and Y. R. Shen, Chem. Phys. Lett. **386**, 144 (2004).

[15] M. R. Querry, D. M. Wieliczka, and D. J. Segelstein, in *Handbook of Optical Constants of Solids II* (Academic Press, New York, 1991), p. 1059.

[16] Y. J. Lai and L. I, Phys. Rev. Lett. **89**, 155002 (2002).